Published by :
http://www.ijert.org

International Journal of Engineering Research & Technology (IJERT)
ISSN: 2278-0181
Vol. 12 Issue 10, October-2023

Effect of Slips and Radiation on Aligned MHD Boundary Layer Flow of Williamson Nanofluid Through Porous Medium

G. Kavitha[1], Ch.Vittal[2], V.Dhanalaxmi[1]

Corresponding author: Vijayalaxmi Tankasala[3]

1. University College of Science, Osmania University, Hyderabad.

2. University College of Science, Saifabad, Osmania University, Hyderabad.

3. N.T.R. Government Degree College for Women, Mahabubnagar, Telangana.

***Abstract*: The present study explores the effect of velocity, thermal and solute slip conditions with aligned magnetic field of Williamson Nano fluid along a stretching sheet through porous medium in the presence of thermal radiation. The object of this study is to examine the phenomena of heat and mass transport caused by thermophoresis and Brownian motion. A set of governing nonlinear partial differential equations for the modelling of boundary layer flow are transformed to ordinary differential equations by using suitable similarity transformations. The resulting coupled non-linear ordinary differential equations are solved numerically with the help of MATLAB. The effect of the flow variable parameters on relevant profiles is calculated and measured qualitatively to get the complete understanding of the present study. To confirm the present analysis, the numerical results are compared with previously published data and they found to be in good agreement. The findings reveal that the velocity profile decreases, the temperature and concentration profiles are increased with increase in inclined angle. Moreover velocity slip diminishes the velocity profile of the fluid and will shows the opposite result in temperature, concentration graphs and both thermal and solutal jumps/slips shows the decreasing nature in temperature and concentration profiles of the fluid as the values of the parameters are increased.**

Keywords: Velocity, thermal and solutal slips - Aligned MHD – Williamson nanofluid- Thermal radiation

INTRODUCTION:

Magnetohydrodynamics, often abbreviated as MHD, is a multidisciplinary field of physics and engineering that combines principles of magnetism and fluid dynamics. It focuses on the study of the behavior of electrically conducting fluids (plasmas, liquid metals and electrolytes) in the presence of magnetic fields. In MHD, the fundamental equations of fluid dynamics are extended to incorporate the effects of electromagnetic forces. This coupling of magnetic and fluids properties has wide-ranging applications in various fields, including astrophysics, fusion energy research, engineering and space exploration. MHD plays a crucial role in understanding various astrophysical phenomena and MHD is integral to the study of controlled nuclear fusion, a potential source of clean and limitless energy. Magnetic confinement techniques like tokamaks and stellarators rely on MHD principles to contain and stabilize high-temperature plasma. MHD technology is employed in aerospace applications and used in the design of electromagnetic pumps and flow control systems, which find applications in metallurgy, cooling of electrical equipment and industrial processes also MHD is employed in the casting and shaping of metals, particularly in the steel industry to control the flow and solidification of molten metals. In the fields of metallurgy and polymer technology, it appears to be frequently utilized. Magnetic drug targeting, astrophysical sensing, and engineering may all benefit from MHD applications [1, 2]. Based on all these significant benefits, analysts and researchers monitor MHD flows on a continuous basis. Metri et al. [3] explore the impact of heat sink/source over MHD forced convective visco-elastic fluid flow subjected to dissipation with porous medium. Akbar et al. [4] numerically studied the influence of MHD heat transport nanofluid flow over a stretched surface for the newheat flux concept. Numerous authors Rashidi et al. [5], Rashidi and Erfani [6], Khedr et al. [7], Fang and Zhang [8], Magyari and Chamkha [9], Ishak et al. [10], Yasin et

International Journal of Engineering Research & Technology (IJERT)
ISSN: 2278-0181
Vol. 12 Issue 10, October-2023

al. [11], Falodun and Omowaye [12], Madhusudan et al. [13] have recently examined the problems on MHD impact of magnetic fields on stretching sheet and various aspects of flow issues. Magnetic effect is said to have a key impact in heat control applications.

A nanofluid is a fluid that contains tiny volumetric amounts of nanometer-sized particles (0–100 nm) called nano-particles. Nanofluids are a class of engineered fluids created by dispersing nanometer-sized solidparticles (typically nanofluid) into a base fluid, which can be a liquid or even a gas. These nanoparticles are usually chosen for their unique properties, such as high thermal conductivity or optical characteristics. The addition of nanoparticles to the base fluid results in a nanoscale colloidal suspension with enhanced properties that can be tailored for specific applications. It has many applications such as to improve the cooling efficiency of electronic devices, such as computer chips and LEDs by enhancing their conductivity and heat dissipation properties. In industrial processes and HVAC system, nanofluids are employed to increases the efficiency of heat exchangers, leading to reduced energy consumption and improved performance. Nanofluids are continually finding new applications across various industries due to their ability to enhance the thermal, electrical, mechanical and optical properties of fluids. Their tunable properties of fluids. Their tunable properties and versatility make them a valuable tool for improving existing technologies and enabling innovative solutions in fields ranging from energy production to healthcare. The dispersion, amorphous movement, thermophoresis effects, Brownian motion, and thermophoresis impacts are a few of these physical properties. The examination of nanofluid flow has piqued the interest of researchers in recent years, due to a rise in applications in many sectors of science & technology, biomechanics, nuclear, and chemical sectors. For instance, food materials (mayonnaise, chocolate, ketchup, alcoholic beverages, yoghurt, milk and apple sauce in liquefied form), chemical materials (paints, cosmetics, pharmaceutical chemicals, toothpastes, oil, reservoirs, shampoos, grease, etc.), and biological materials (synovial fluid, syrups, vaccines, blood, etc.). The term nanofluid was first coined by Choi [14]. The thermal conductivity of copper nanoparticles embedded in a nanofluid of ethylene glycol was explored by Eastmann et al. [15]. Since then, thermophoresis and Brownian diffusion demonstrations have fueled the advancement of mathematical modeling of nanofluids. The free convective flow of a nanoliquid was investigated by Kuznetsov and Nield [16] using an analytical approach. The stagnation-point flow of a nanofluid toward a non-linear stretching sheet was explored with Anwar et al. [17]. Azimi and Riazi [18] discussed heat transmission between two parallel disks of Go-water Nanofluid. Bhargava et al. [19] described an effective hybrid method for modeling MHD nanofluid flow through a permeable stretched sheet. [20] Raza et al. scrutinized MHD Flow of nano-Williamson liquid caused via multiple slips on a stretched plate. Khan [21] investigated the stability of magneto convective flow of SiO2–MoS2/C2H6O2 hybrid nanoliquids using a shrinking/stretching wedge. Chamkka et al. [22] investigated the laminar MHD mixed convection flow of a nanoliquid over a stretched permeable area with heat production or absorption. Turkyilmazoglu [23] investigated an accurate analytical solution for heat and mass transport in nanofluids with MHD slip flow. Wubshet and Shankar [24] studied the flow and heat transfer of a nanofluid via a permeable stretched sheet under a variety of boundary conditions, including velocity, temperature, and solutal slip. Nagendra et al. [25] investigated the numerical simulation of hydromagnetic heat and mass transport in a nano-Williamson liquid passing through a vertical plate through thermal and momentum slip effects. Garoosi et al. [26] studied numerical modeling of natural convection in heat exchangers utilizing the Buongiorno model. Konda et al. [27] analyzed the performance of a non-uniform heat sink/source on the MHD boundary layer flow and melting heat transport of a Williamson nanoliquid in a porous media. Yahaya et al. [28] explored nanofluid hydromagnetic slip flow with thermal stratification and convective heating. Acharya et al. [29] investigated the impact of numerous slips and chemical reactions on the radiative MHD Williamson nanoliquid flow in porous media: A computational approach. Mishra and Mathur [30] used a semi-analytical technique to investigate Williamson nanofluid flow in porous media with melting heat transport boundary conditions. Asogwa et al. [31] investigated the comparative analysis of water-based Al2O3 nanoparticles via H2O-based CuO nanoparticles through heat transport toward an exponentially accelerated radiative Riga plate area. Warke et al. [32] investigated nonlinear radiation through magneto micro polar stagnation point flow over a heated stretching sheet using a numerical investigation.

International Journal of Engineering Research & Technology (IJERT)
ISSN: 2278-0181
Vol. 12 Issue 10, October-2023

Thermal radiation, which is the emission of electromagnetic radiation from a body due to its temperature, has several important applications in scientific research and it encompasses electric power, food, solar cell panels, gas turbines, different propulsion mechanisms for aero planes, and the medical sector. The impact of radiation and mixed convection on nanofluid flow over a vertical plate with melting heat transport was investigated by Mahanthesh et al. [33]. FazleMabood et al. [34] investigated the radiation impact on MHD Williamson nanoliquid flow with a heated surface. On a shrinking/stretching porous sheet, thermo-diffusion and radiation effects on Williamson nanofluid were investigated by Bhatti and Rashidi [35]. The influence of radiation on nanofluid flow across a stretched surface was inspected by Krishnamurthy et al. [36], Dulal Pal et al. [37], Ghadikolaei et al. [38], and Almakki et al. [39]. This work is based on several recent articles as [40–47].

Slip conditions typically refer to the behavior of the fluid at the fluid-solid interface. Slip boundary conditions are classified into no-slip conditions (where the fluid velocity at the interface is zero) and slip conditions (where the fluid velocity at the interface is not zero). Understanding and how slip conditions affect the flow of nanofluid through a porous medium involves considering factors like fluid dynamic, heat transfer and slip conditions can significantly impact the velocity profile of the fluid within the porous medium. Silp condition generally imply a non-zero velocity at the fluid-porous medium interface. This affects the flow pattern and can lead to changes in flow rate and pressure distribution.

Inspired by above reputed researchers and importance of slips on nanofluids, the present work discusses the effect of slips on Williamson nanofluid flowing via a porous media in the presence of aligned magnetic field with a constant stretching sheet. According to the aforementioned literatures, no study has been conducted on aligned MHD nanofluid via a stretching sheet when thermal radiation and slip conditions are present. The solution of coupled nonlinear equations is obtained by numerical computing and for numerous values of physical restrictions, the consequence of dimensionless parameters has been evoked. The originality of this observation is to consider the behavior of the radiation, velocity, thermal and solutal slips on aligned MHD boundary layer flow through heat and mass transport in a Williamson nanoliquid with porous media.

FORMULATION OF THE PROBLEM:

Assume that the steady-state two dimensional incompressible MHD Williamson nanofluid flow toward a horizontal stretching sheet under the influence of aligned magnetic field through the porous medium and with the effect of thermal radiation and slips. From the physical model of the problem which demonstrated in Figure 1 the plate is extended along the direction of X axis and Y axis is the direction normal to the stretching sheet. Along with these the fluid is permitted by an aligned magnetic field. Plate velocity is $U_w(x) = bx,\ (b > 0)$, the wall temperature T_w and the nanoparticle fraction C_w are assumed constant at the stretching surface. When y tends to infinity, the ambient values of temperature and nanoparticle fraction are denoted by T_w and C_w, respectively. The boundary layer equations[48] for the flow of two-dimensional under the above constraints and occurrence of aligned magnetic field and thermal radiation are

$$\frac{\partial u}{\partial x} + \frac{\partial v}{\partial y} = 0 \qquad (1)$$

$$u\frac{\partial u}{\partial x} + v\frac{\partial u}{\partial y} = \nu\frac{\partial^2 u}{\partial y^2} + \sqrt{2}\gamma\Gamma\frac{\partial u}{\partial y}\frac{\partial^2 u}{\partial y^2} - \frac{\sigma B_0^2}{\rho}Sin^2\gamma u - \frac{\gamma}{k}u \qquad (2)$$

$$u\frac{\partial T}{\partial x} + v\frac{\partial T}{\partial y} = \alpha\frac{\partial^2 T}{\partial y^2} + \tau\left\{D_B\frac{\partial C}{\partial y}\frac{\partial T}{\partial y} + \frac{D_T}{T_\infty}\left(\frac{\partial T}{\partial y}\right)^2\right\} - \frac{1}{(\rho C)_{nf}}\frac{\partial q_r}{\partial y} \qquad (3)$$

International Journal of Engineering Research & Technology (IJERT)
ISSN: 2278-0181
Vol. 12 Issue 10, October-2023

$$u\frac{\partial C}{\partial x}+v\frac{\partial C}{\partial y}=D_B\frac{\partial^2 C}{\partial y^2}+\frac{D_T}{T_\infty}\frac{\partial^2 T}{\partial y^2} \qquad (4)$$

The following are subject to the appropriate conditions at the boundary

$$u=u_w+A^*\mu\left(\frac{\partial u}{\partial y}\right),\quad v=0,\quad T=T_w+B^*\left(\frac{\partial T}{\partial y}\right),\quad C=C_w+C^*\left(\frac{\partial C}{\partial y}\right)\quad at\ \ y=0$$

$$u\to 0,\qquad T=T_\infty,\ \ C=C_\infty,\quad as\ y\to\infty \qquad (5)$$

Where $A^*,\ B^*\ and\ C^*$ are velocity, thermal and solutal slip factors

Using the Rosseland [30] approximation the radiative heat flux is simplified as:

$$q_r=-\frac{4\sigma_i}{3K^*}\frac{\partial T^4}{\partial y} \cdots\cdots\cdots\cdots (6)$$

We assume that the temperature differences within the flow region, namely, the term T^4can be expressed as a linear function of temperature. The best linear approximation of T^4 is obtained by expanding it in a Taylor series about T_∞ is

$$T^4=T_\infty^4+4T_\infty^3(T-T_\infty)+6T_\infty^2(T-T_\infty)^2+\cdots\cdots\cdots\cdots (7)$$

Neglecting higher order terms of $(T-T_\infty)$ from equation (7) and attained as

$$T^4\cong 4TT_\infty^3-3T_\infty^3 \cdots\cdots\cdots\cdots (8)$$

Using equation (9) into equation (7) we get

$$q_r=-\frac{16\sigma_i T_\infty^3}{3K^*}\frac{\partial T}{\partial y} \cdots\cdots\cdots\cdots (9)$$

The modified equation of (3) by the assistance of equation (9) is

$$u\frac{\partial T}{\partial x}+v\frac{\partial T}{\partial y}=\alpha\frac{\partial^2 T}{\partial y^2}+\tau\left\{D_B\frac{\partial C}{\partial y}\frac{\partial T}{\partial y}+\frac{D_T}{T_\infty}\left(\frac{\partial T}{\partial y}\right)^2\right\}+\left(\frac{16\sigma_i T_\infty^3}{3(\rho C_p)_f K^*}\frac{\partial^2 T}{\partial y^2}\right) \qquad (10)$$

Employing the following similarity Transformations:

$$\eta=y\sqrt{\frac{b}{\gamma}},\ \ u=bxf'(\eta),\ \ v=-\sqrt{b\gamma}f,\theta(\eta)=\frac{T-T_\infty}{T_w-T_\infty},\ \ \phi(\eta)=\frac{C-C_\infty}{C_w-C_\infty} \qquad (11)$$

Using transformations (11) in equations (2), (4) and (8) subject to the constraints in (5) will be in the following form:

$$f'''+\lambda f''f'''+ff''-(f')^2-(Sin^2\gamma M+k)f'=0 \qquad (12)$$

$$\left(\frac{3+4R}{3}\right)\theta''+Pr.f\theta'+\frac{Nc}{(Le)(Nbt)}(\theta')^2-2Pr.f'\theta+\left(\frac{Nc}{Le}\right)\theta'\phi'=0 \qquad (13)$$

$$\phi''+Scf\phi'+\left(\frac{1}{Nbt}\right)\theta''=0 \qquad (14)$$

The governing parameters are

International Journal of Engineering Research & Technology (IJERT)
ISSN: 2278-0181
Vol. 12 Issue 10, October-2023

$\lambda = \Gamma x\sqrt{\frac{2b^3}{\gamma}}$, $Le = \frac{\alpha}{D_B}$ $M = \frac{\sigma B_0^2}{b\rho}$, $Pr = \frac{\gamma \rho C_p}{\kappa}$, $R = \frac{4\sigma^* T_\infty^3}{k\kappa}$, $k = \frac{\gamma}{bk}$, $Nc = \frac{(\rho c)_p}{(\rho c)_f}(C_w - C_\infty)$, $Nbt = \frac{T_\infty D_B (C_w - C_\infty)}{D_T (T_w - T_\infty)}$, $Sc = \frac{\gamma}{D_B}$,

Where f, θ and φ are functions of η and prime labels differentiation w.r.to η. The equivalent transformed boundary conditions are

$$f(0) = 0, \quad f'(0) = 1 + Af''(0), \quad \theta(0) = 1 + B\theta'(0), \quad \phi(0) = 1 + C\phi'(0) \quad at \ \eta = 0$$

$$f'(\infty) = 0, \ \theta(\infty) = 0, \ \varphi(\infty) = 0 \qquad (15)$$

The quantities of physical interest are described as the coefficient of friction kin-friction coefficient Cf, the local Nusselt numberNu_x and the Sherwood number Sh_x are expressed as follows

$C_f = \frac{\tau_w}{\rho U_w^2}$, $Nu_x = \frac{x q_v}{\kappa (T_f - T_\infty)}$ and $Sh_x = \frac{q_m x}{D_B (C_w - C_\infty)}$ (16)

Where τ_w is the shear stress, q_w is the heat flux and q_m is the mass flux volume fraction of the nanoparticle at the plate surface, which are specified by

$\tau_w = \mu\left[\frac{\partial u}{\partial y} + \frac{\Gamma}{\sqrt{2}}\left(\frac{\partial u}{\partial y}\right)^2\right]$, $q_w = -k\left(\frac{\partial T}{\partial y}\right)_{y=0}$ and $q_m = -k\left(\frac{\partial C}{\partial y}\right)_{y=0}$ (17)

Finally using equations (17) and (11), equation (16) becomes

$$Re_x^{\frac{1}{2}} Cf = f''(0) + \frac{\lambda}{2} f(0)''^2, \ Re_x^{\frac{-1}{2}} Nu_x = -\theta'(0) \ and \ Re_x^{\frac{-1}{2}} Sh_x = -\phi'(0) \qquad (18)$$

METHOD OF SOLUTION:

The non-linear ordinary differential equations (12) to (14) together with boundary conditions (15) are solved numerically by an implicit finite difference scheme namely the Keller Box method and the following steps are involved in this method.

• Reduce the ordinary differential equations to a system of first order equations.

• Write the difference equations for ordinary differential equations using central differences.

• Linearize the algebraic equations by Newtons method, and write them in matrix vector form.

• Solve the linear system by the block tri-diagonal elimination technique. The accuracy of the method is depends on the appropriate initial guesses. We made an initial guesses are as follows.

$$f(\eta) = \left(\frac{1}{1+A}\right)(1 - e^{-\eta}), \quad \theta(\eta) = \left(\frac{1}{1+B}\right)e^{-\eta}, \quad \varphi(\eta) = \left(\frac{1}{1+C}\right)e^{-\eta}$$

The choices of the above initial guesses depend on the convergence criteria and the transformed boundary conditions of equations (15). The step size 0.01 is used to obtain the numerical solution with six decimal place accuracy as the criterion of convergence.

RESULTS AND DISCUSSION:

We used the Kellor-Box method to get a physical understanding of the present investigation of aligned MHD heat and mass transport Willamson nanofluid flow with thermal radiation, porous medium and slips. The findings are autherizes the effect of various non-dimensional factors on the velocity, temperature and concentration profiles in addition to coefficient of friction factor, heat transport and mass transfer using tables and diagrams. In this investigation the non-dimensional parameter values $\lambda = 0.5, M = 0.3, k = 0.2, \beta = 1.0, Pr = 7.0, Nc = 2.5, Nbt = 2.0, Le = 10, Sc = 5.0, R = 0.5, \gamma = \frac{\Pi}{2}, A = 0.25, B = 0.5, C =$

International Journal of Engineering Research & Technology (IJERT)
ISSN: 2278-0181
Vol. 12 Issue 10, October-2023

0.5 were used. To validate the current numerical outcomes, a comparison with Y. Dharmendar Reddy et al was performed and found in good agreement, as shown in Table I, II and III.

Table I: Comparison of skin friction $(-f''(0))$ values for various values of δ, λ, M, k when

$$\beta = 1.0, Pr = 7.0, Nc = 2.5, Nbt = 2.0, Le = 10, Sc = 5.0, R = 0.5, \gamma = \frac{\Pi}{2}, B = 0, C = 0$$

δ	λ	M	k	Y. Dharmendar Reddy et al	Present study
0.25	0.5	0.3	0.2	-1.1551	-1.155109
0.75				-0.6689	-0.668911
1.25				-0.4694	-0.469408
1.75				-0.3598	-0.359812
	0.0			-0.7201	-0.720121
	0.3			-0.7903	-0.790365
	0.5			-0.8461	-0.846174
	0.7			-0.9630	-0.963097
		0.0		0.7062	0.706204
		0.2		0.8004	0.800456
		0.4		0.8911	0.891132
		0.8		1.0684	1.068461
			0.1	0.8004	0.800455
			0.3	0.8911	0.891189
			0.5	0.9799	0.979941
			0.7	1.0684	1.068477

Table II: Comparison of $-\theta'(0)$ and $-\phi'(0)$ for various values of δ, β, λ, Pr, Nc, Nbt when $Le = 10$, $Sc = 5$, $M = 0.5$, $R = 0.5$, $k = 0.2$

δ	β	λ	Pr	Nc	Nbt	Y. Dharmendar Reddy et al $-\theta'(0)$	Present study	Y. Dharmendar Reddy et al $-\phi'(0)$	Present study
0.25	1.0	0.5	7	2.5	2	1.3357	1.335709	0.8086	0.808633
0.75						1.0444	1.044465	0.7169	0.716909
1.25						0.9168	0.91689	0.6239	0.623902
1.75						0.8244	0.824424	0.5558	0.555834
	0.2					1.8752	1.875287	0.5016	0.501683
	0.4					1.6095	1.609550	0.5999	0.599929

International Journal of Engineering Research & Technology (IJERT)
ISSN: 2278-0181
Vol. 12 Issue 10, October-2023

	0.6					1.4098	1.409829	0.6739	0.673931
	0.8					1.2541	1.254128	0.7315	0.731522
		0.0				1.1461	1.146148	0.8014	0.801449
		0.3				1.1386	1.138693	0.7874	0.787431
		0.5				1.1294	1.129475	0.7777	0.777785
		0.7				1.1180	1.118008	0.7633	0.763344
			4			0.8074	0.807481	0.9135	0.913519
			6			1.0313	1.031336	0.8198	0.819811
			8			1.2208	1.220807	0.7379	0.737962
			10			1.3882	1.388211	0.6639	0.663907
				5		1.0819	1.081939	0.7988	0.798881
				10		0.9932	0.993299	0.8377	0.837777
				15		0.9129	0.912962	0.8726	0.872638
				20		0.8404	0.840404	0.9038	0.903842
					0.3	1.0939	1.093977	-1.4932	-1.493254
					0.4	1.1041	1.104111	-0.8427	-0.842766
					0.6	1.1145	1.114508	-0.1780	-0.178031
					0.9	1.1216	1.121639	0.2734	0.273419

Table III: Comparison of $-\theta'(0)$ and $-\phi'(0)$ for different values of $Le,\ Sc,\ M,\ R,\ k$

Le	Sc	M	R	k	Y. Dharmendar Reddy et al $-\theta'(0)$	Present study	Y. Dharmendar Reddy et al $-\phi'(0)$	Present study
1	5	0.3	0.5	0.2	0.7752	0.775211	0.9315	0.931511
1.5					0.8879	0.887905	0.8834	0.883408
2.0					0.9520	0.952026	0.8556	0.855695
2.5					0.9932	0.9932	0.8377	0.837729
	2				1.1487	1.148738	0.1866	0.186633
	4				1.1345	1.134547	0.6090	0.609008
	6				1.1251	1.125105	0.9294	0.929461
	8				1.1180	1.118094	1.1970	1.197039
		0.0			1.1526	1.152639	0.8160	0.816009
		0.2			1.1369	1.136929	0.7899	0.789922
		0.4			1.1221	1.122122	0.7666	0.766686
		0.8			1.0944	1.094475	0.7228	0.722822
			0.1		1.3874	1.387408	0.6645	0.664571
			0.3		1.2406	1.240623	0.7293	0.729388

International Journal of Engineering Research & Technology (IJERT)
ISSN: 2278-0181
Vol. 12 Issue 10, October-2023

			0.5		1.1294	1.129463	0.7777	0.777731
			0.9		0.9695	0.969544	0.8459	0.845905
				0.1	1.1369	1.136911	0.7899	0.789911
				0.3	1.1221	1.122180	0.7660	0.766099
				0.5	1.1080	1.108088	0.7437	0.743739
				0.7	1.0944	1.094431	0.7228	0.722845

Figures 2, 3 and 4 discloses the consequences of the Williamson parameter $\boldsymbol{\lambda}$ on the profiles of velocity, temperature and concentration. It is noticed that growing values of $\boldsymbol{\lambda}$ diminishes the fluid velocity and increases the temperature and concentration distributions. Effect of magnetic parameter $\boldsymbol{M}$ on the velocity profile is displayed in Figure 5 by keeping the other parameters fixed. It is observed that an increase in magnetic field parameter decreases the velocity due to increasing magnetic field parameter improves the opposite force to the flow of nanofluid direction called 'Lorentz force' and this force opposes the motion of the nanofluid which results in decreases the velocity of the fluid. Figure 6 shows the influence of magnetic field parameter $\boldsymbol{M}$ on the thermal field. Transverse magnetic field has increased the thermal boundary layer thickness, so it causes the temperature increment in the boundary layer when it increases. It can be seen from Figure 7 the increase of magnetic parameter $\boldsymbol{M}$ increases the magnitude of concentration profiles. Figures 8, 9 and 10 are plotted to observe the effects of angle of inclination on velocity, temperature and concentration profiles respectively. It is clear from figures that the temperature and concentration profiles are increased with increase in inclined angle, this enhancement is due to the raise in the magnetic field parameter. The velocity profile decreases with the increase of aligned angle. It may happen with the increase in angle of inclination, causes to strengthen the applied magnetic field. Because of enhanced magnetic field an opposite force is produced to the flow, called Lorentz force. Consequently the velocity profile decreases. It is also seen that for the $\boldsymbol{\gamma = 0}$ the magnetic field is not effected on the velocity profile while maximum resistance is offered for the fluid particles when $\boldsymbol{\gamma = \frac{\pi}{2}}$. The porosity parameter $\boldsymbol{k}$ is the dimensionless number which defines the level of porosity within a fluid. Figure 11, 12 and 13 illustrates the momentum, heat and mass profile for different values of porosity parameter $\boldsymbol{k}$. With increasing permeability parameter, the resistance to the fluid motion increases and hence velocity decreases. For increased values of the porosity parameter $\boldsymbol{k}$, temperature and concentration profiles increase, and the opposite behavior is seen in the velocity profile. Porosity parameter $\boldsymbol{k}$ grows a resistance force (due to the increase in the pores in the fluid) that works conversely to the flow field and enhances the thermal and solutal boundary layer thickness. Figure 14 demonstrates the variation of temperature with respect to radiation parameter $\boldsymbol{R}$. When the Rosseland radiative absorptivity k^* decreases, the divergence of the radiative heat flux $\partial qr / \partial y$ increases, which leads to increases the rate of radiative heat transfer to the fluid at the surface, i.e., it provides more heat to the fluid which causes the fluid temperature to increase. Hence, the temperature profile as well as thermal boundary layer thickness increases as the value of thermal radiation increases. The variation in Prandtl number $\boldsymbol{Pr}$ on temperature is shown in Figure 15. The temperature field decreases when Pr increases. It is obvious that, an increase in the values of Pr reduces the thermal diffusivity, therefore thermal boundary layer thickness is a decreasing function of Pr. Figure 16 is demonstrated to examine the effect of $\boldsymbol{Nc}$ on the temperature profile. When the increment is done in the parametric value of heat capacity ratio, the curves of temperature profile gave an increasing behavior. So, temperature was increased with increasing the heat capacity ratio. In Figure 17, diffusivity ratio parameter $\boldsymbol{Nbt}$ is depicted to show its behaviour on concentration profile. A significant downfall in the curve of concentration profile is obtained when gradual increase is done in diffusivity ratio parameter $\boldsymbol{Nbt}$.

International Journal of Engineering Research & Technology (IJERT)
ISSN: 2278-0181
Vol. 12 Issue 10, October-2023

Figure 18 is drawn to summarize the consequence of Lewis number Le on the temperature profile. The curve pattern shows that the increasing Lewis number markedly decreased the temperature profile due to a higher value of Lewis number represents a lower nanoparticle diffusivity and a higher thermal diffusivity. If $Le > 1$, the thermal diffusion rate exceeds the Brownian diffusion rate. Lower Brownian diffusion leads to less mass transfer rate, as a result, the nanoparticle volume fraction graph and the concentration boundary layer thickness decrease. Behavior of concentration profile regarding Schmidt number Sc is depicted in Figure 19. When parametrical values of Sc are boosted up, a significant decrease is resulted in concentration profile. The effects of velocity slip parameter A on the dimensionless velocity, temperature and concentration is displayed in Figures 20, 21 and 22 respectively. From the figures velocity decreases with increase in the values of slip parameter, velocity distribution is found to decrease along the boundary layer, but the effect reverse in the case of temperature and concentration profiles. Physically, in the presence of slip the slipping fluid shows a decrease in the surface skin friction between the stretching sheet and the fluid because not all the pulling force of the stretching surface can be transferred to the fluid. So the flow velocity decreases when the value of A increases. As the slip parameter increases in magnitude the friction force is occurred which allows more fluid to slip past the sheet, the flow slows down for distances close to the sheet and the temperature and concentration enhances due to the occurrence of the force. The influence of thermal jump parameter B on the temperature and concentration profiles is shown in Figures 23, 24 which describes that both the fluid temperature and concentration decreases on increasing thermal jump parameter in the boundary layer region. As the effect increases more fluid will be transferred to the thermal boundary layer. Hence, rate of heat and mass transfer will increase and as a result of this, the thermal and solutal boundary layer decreases. From Figure 25 we can observe the variation of concentration with respect to solutal slip parameter C. As it can be seen from the graph, increasing in the concentration slip parameter C, the concentration profile is decreasing.

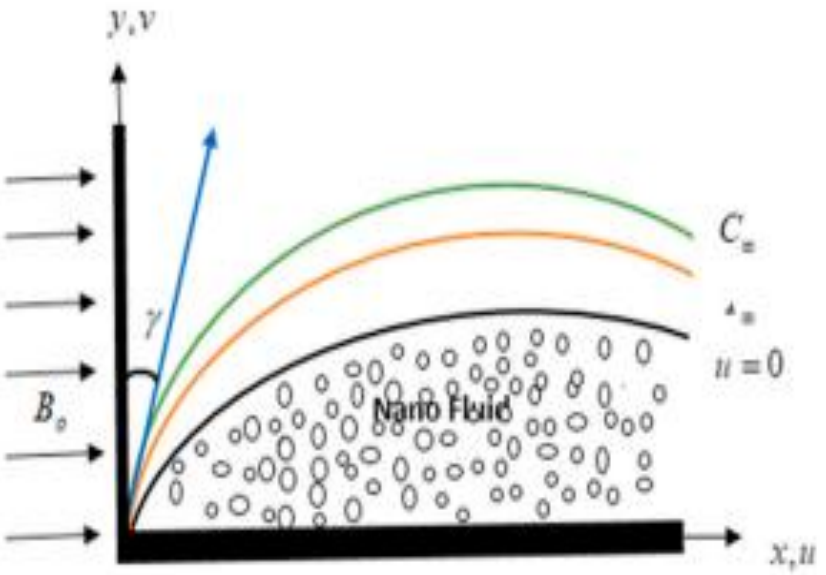

Fig.1. Physical model of the problem

International Journal of Engineering Research & Technology (IJERT)
ISSN: 2278-0181
Vol. 12 Issue 10, October-2023

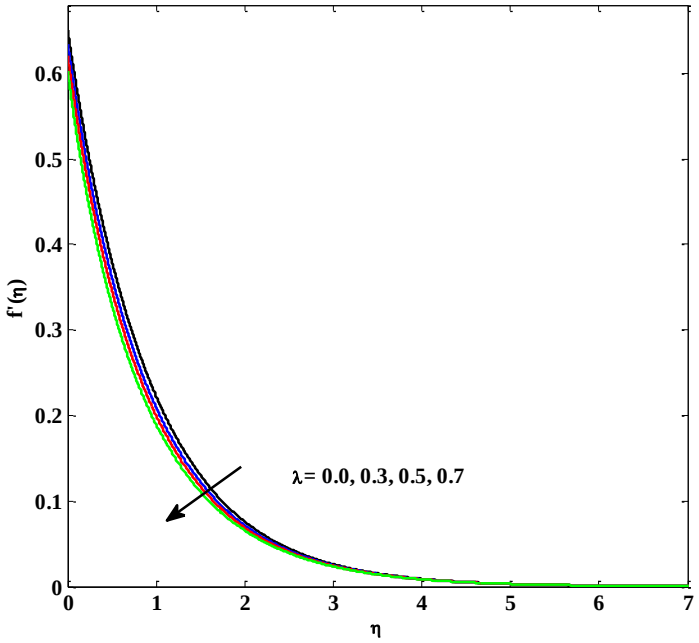

Fig.2. $f'(\eta)$ for picked values of λ

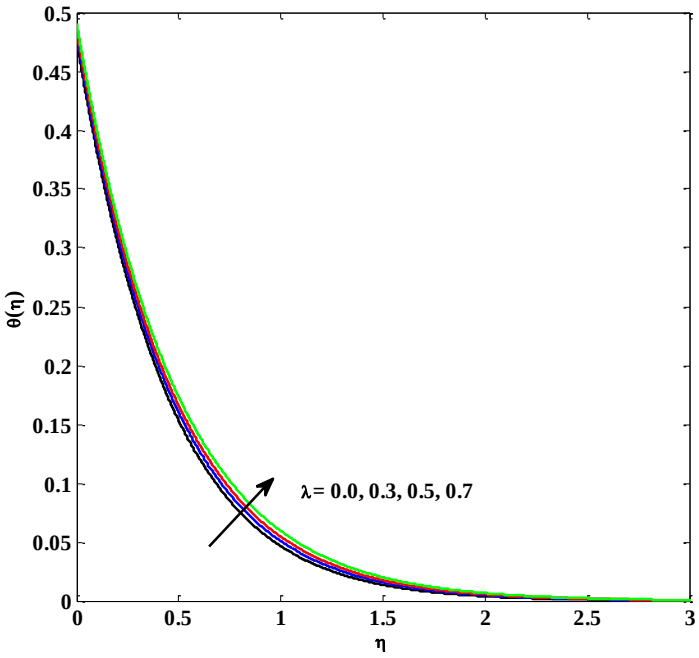

Fig. 3. $\theta(\eta)$ for picked values of λ

International Journal of Engineering Research & Technology (IJERT)
ISSN: 2278-0181
Vol. 12 Issue 10, October-2023

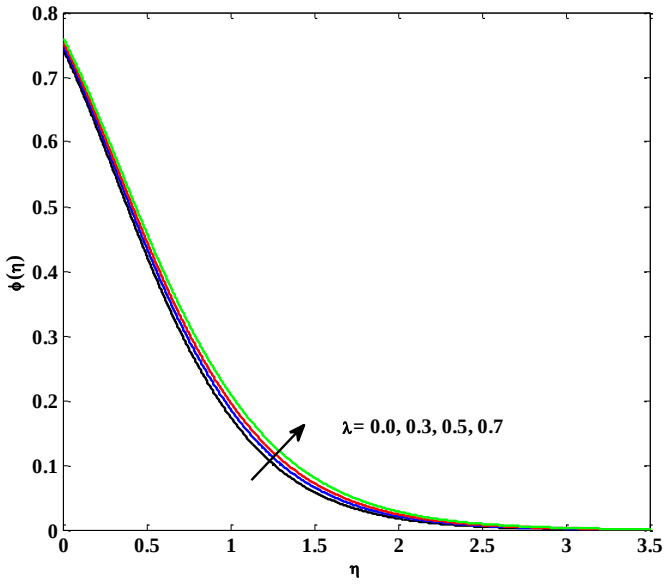

Fig. 4. $\varphi(\eta)$ for picked values of λ

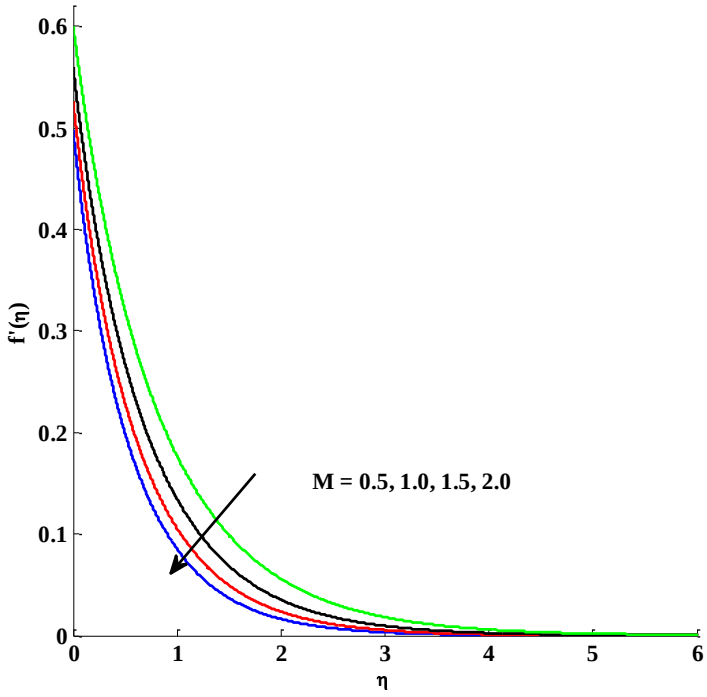

Fig. 5. $f'(\eta)$ for picked values of M

International Journal of Engineering Research & Technology (IJERT)
ISSN: 2278-0181
Vol. 12 Issue 10, October-2023

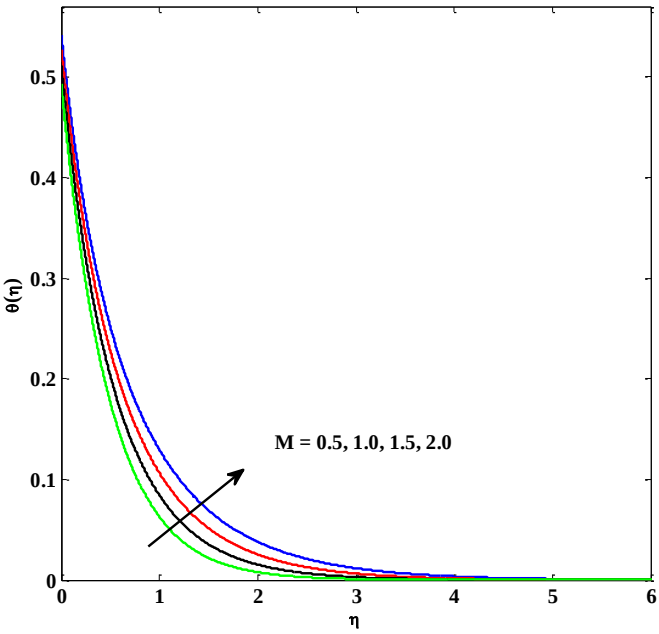

Fig. 6. $\theta(\eta)$ for picked values of M

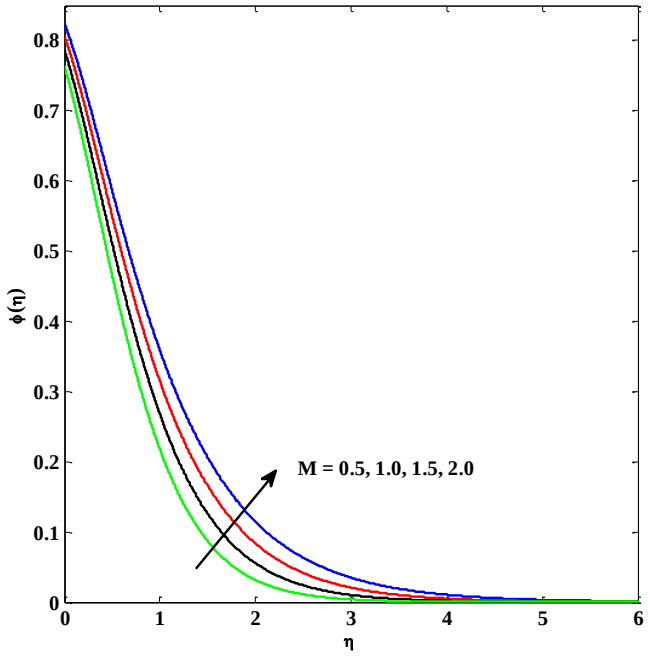

Fig. 7. $\varphi(\eta)$ for picked values of M

International Journal of Engineering Research & Technology (IJERT)
ISSN: 2278-0181
Vol. 12 Issue 10, October-2023

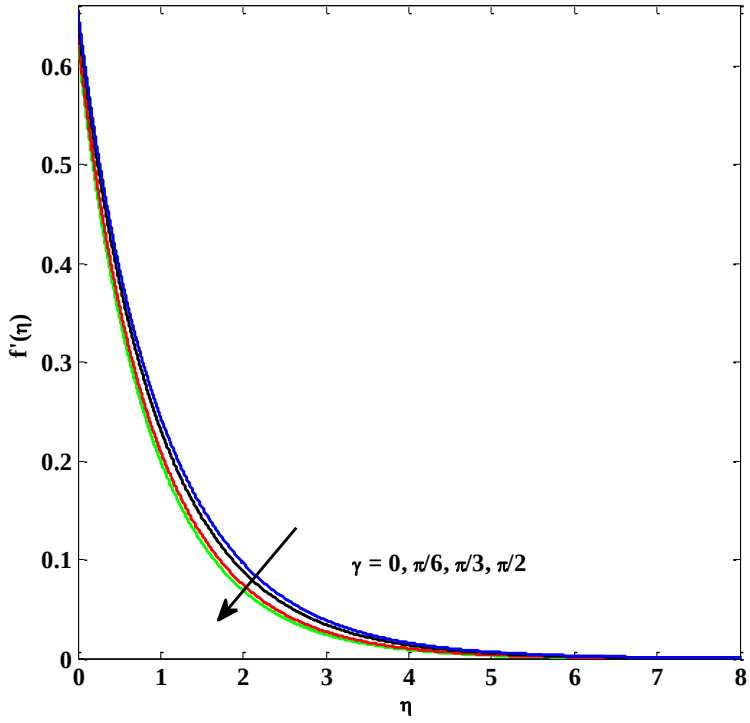

Fig. 8. $f'(\eta)$ for picked values of γ

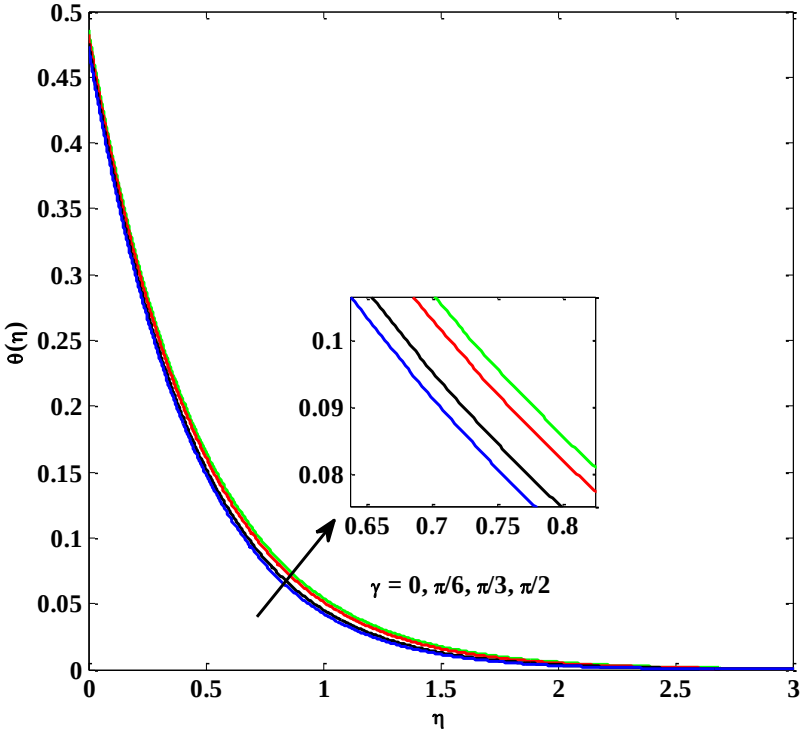

Fig. 9. $\theta(\eta)$ for picked values of γ

International Journal of Engineering Research & Technology (IJERT)
ISSN: 2278-0181
Vol. 12 Issue 10, October-2023

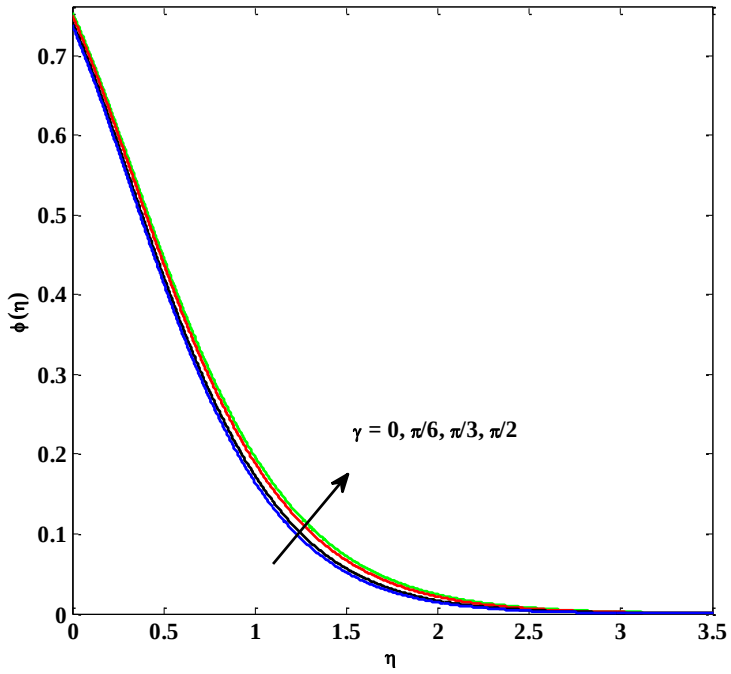

Fig. 10. $\varphi(\eta)$ for picked values of γ

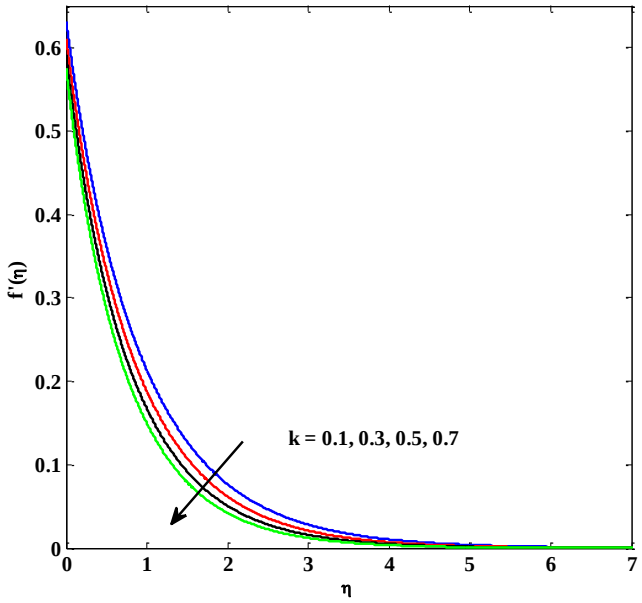

Fig. 11. $f'(\eta)$ for picked values of k

International Journal of Engineering Research & Technology (IJERT)
ISSN: 2278-0181
Vol. 12 Issue 10, October-2023

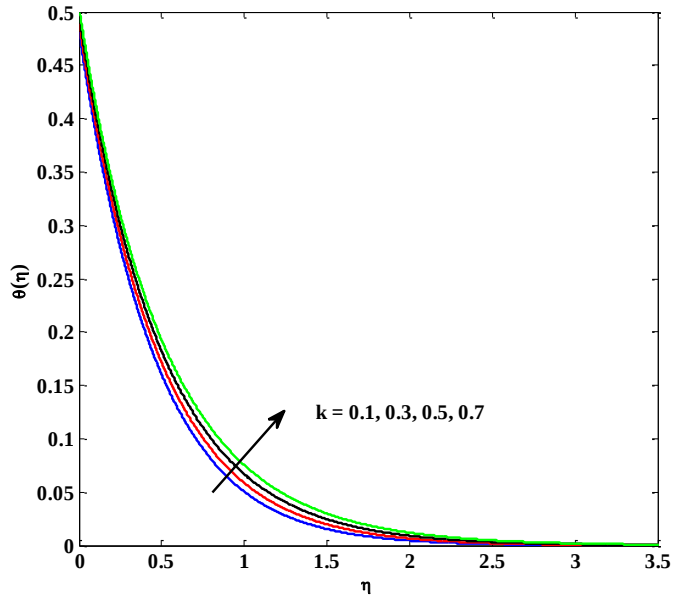

Fig. 12. $\theta(\eta)$ for picked values of k

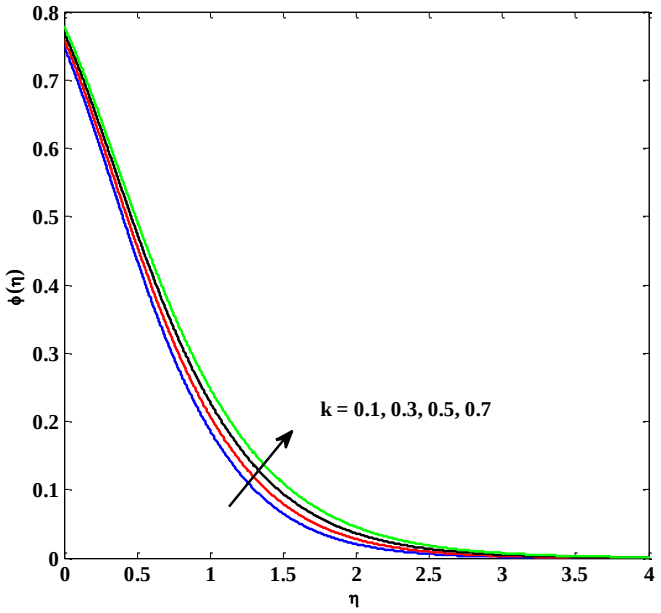

Fig. 13. $\varphi(\eta)$ for picked values of k

International Journal of Engineering Research & Technology (IJERT)
ISSN: 2278-0181
Vol. 12 Issue 10, October-2023

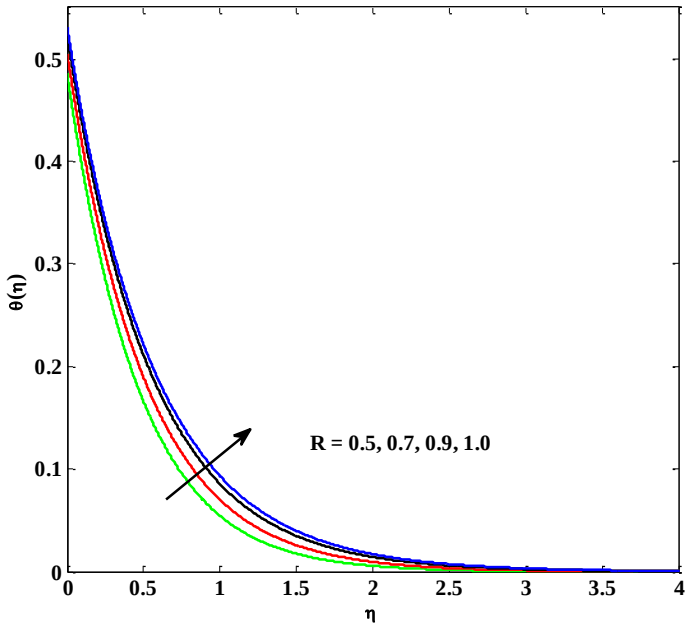

Fig. 14. $\theta(\eta)$ for picked values of R

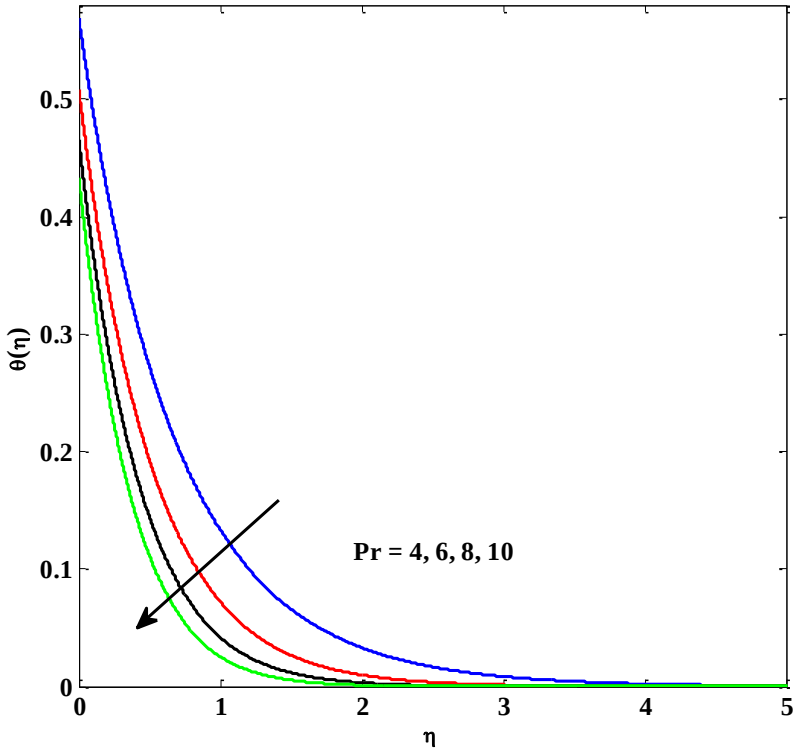

Fig. 15. $\theta(\eta)$ for picked values of Pr

International Journal of Engineering Research & Technology (IJERT)
ISSN: 2278-0181
Vol. 12 Issue 10, October-2023

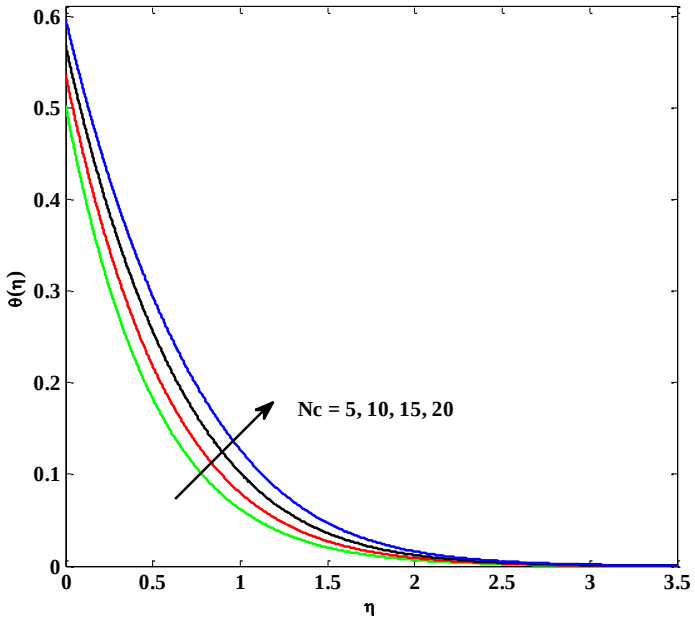

Fig. 16. $\theta(\eta)$ for picked values of Nc

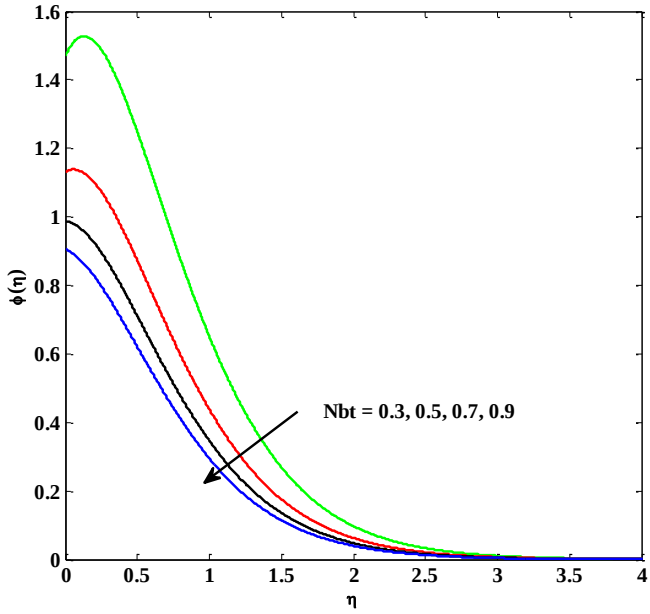

Fig. 17. $\varphi(\eta)$ for picked values of Nbt

International Journal of Engineering Research & Technology (IJERT)
ISSN: 2278-0181
Vol. 12 Issue 10, October-2023

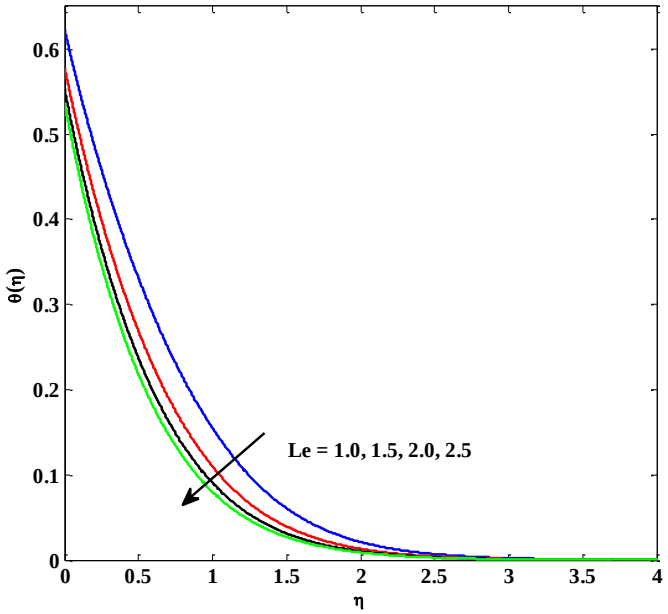

Fig. 18. $\varphi(\eta)$ for picked values of Le

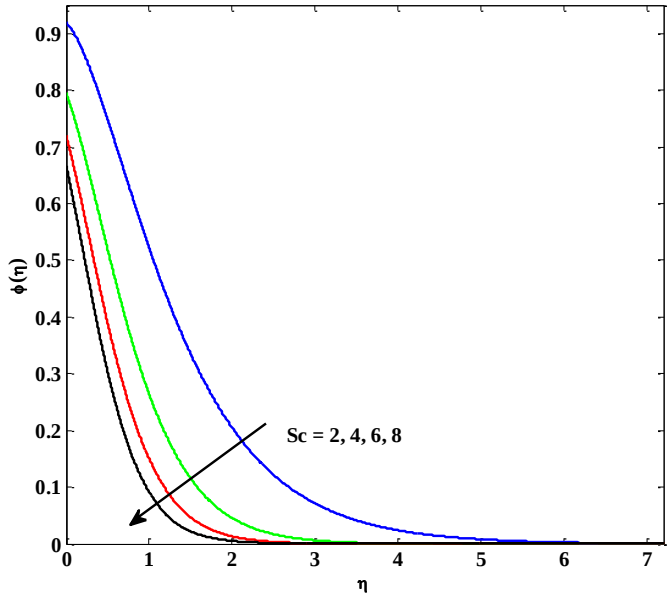

Fig. 19. $\varphi(\eta)$ for picked values of Sc

International Journal of Engineering Research & Technology (IJERT)
ISSN: 2278-0181
Vol. 12 Issue 10, October-2023

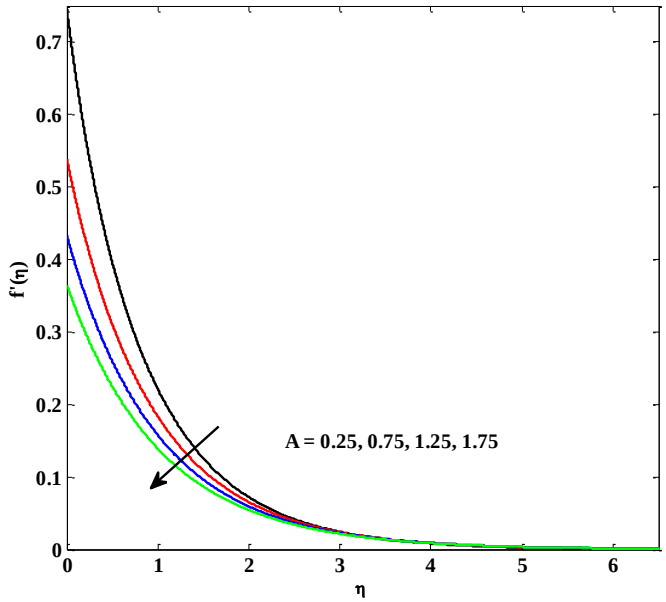

Fig. 20. $f'(\eta)$ for picked values of A

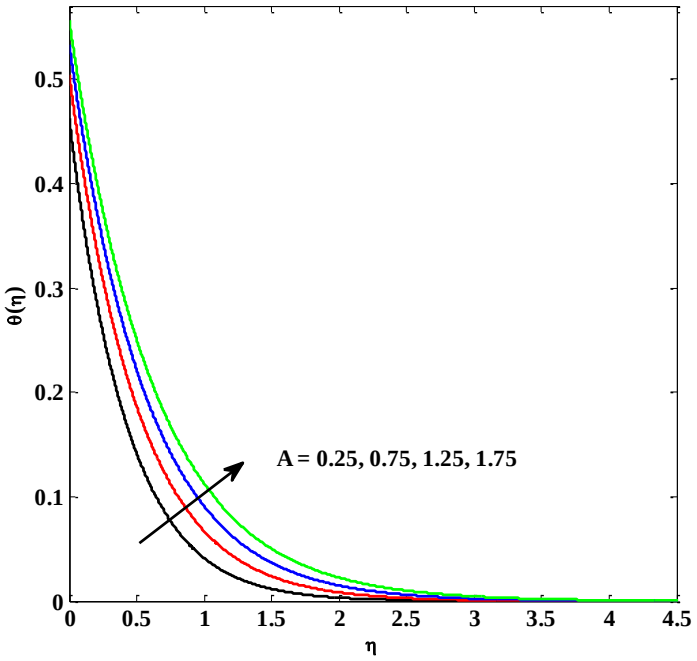

Fig. 21. $\theta(\eta)$ for picked values of A

International Journal of Engineering Research & Technology (IJERT)
ISSN: 2278-0181
Vol. 12 Issue 10, October-2023

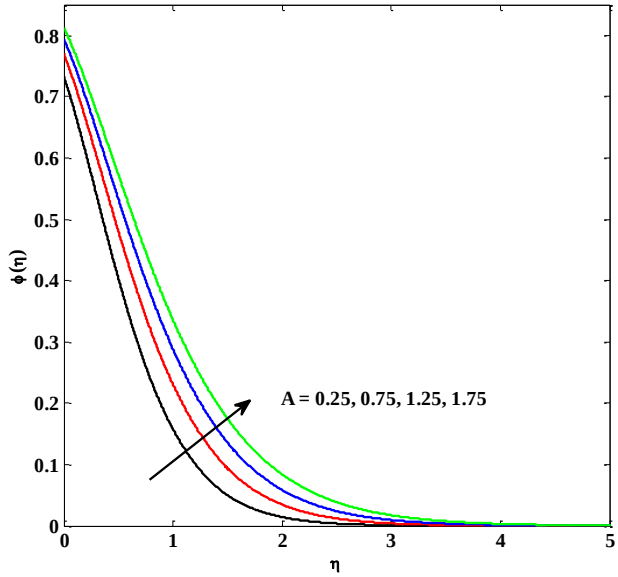

Fig. 22. $\varphi(\eta)$ for picked values of A

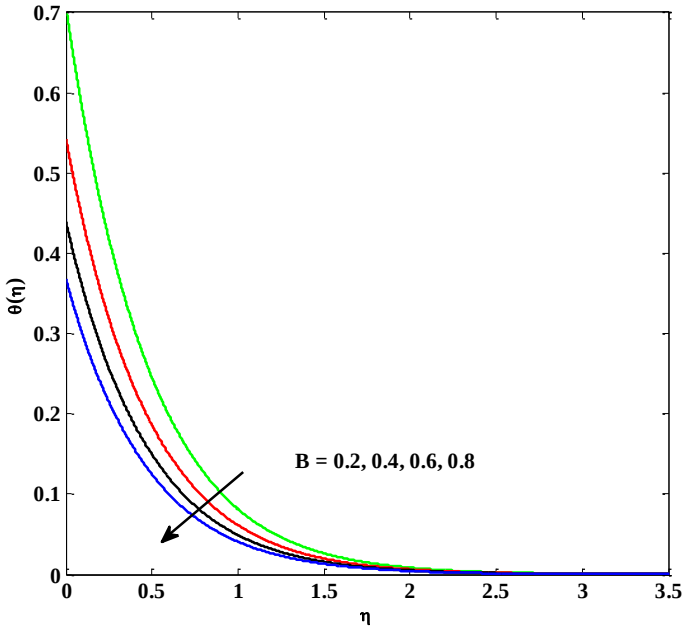

Fig. 23. $\theta(\eta)$ for picked values of B

International Journal of Engineering Research & Technology (IJERT)
ISSN: 2278-0181
Vol. 12 Issue 10, October-2023

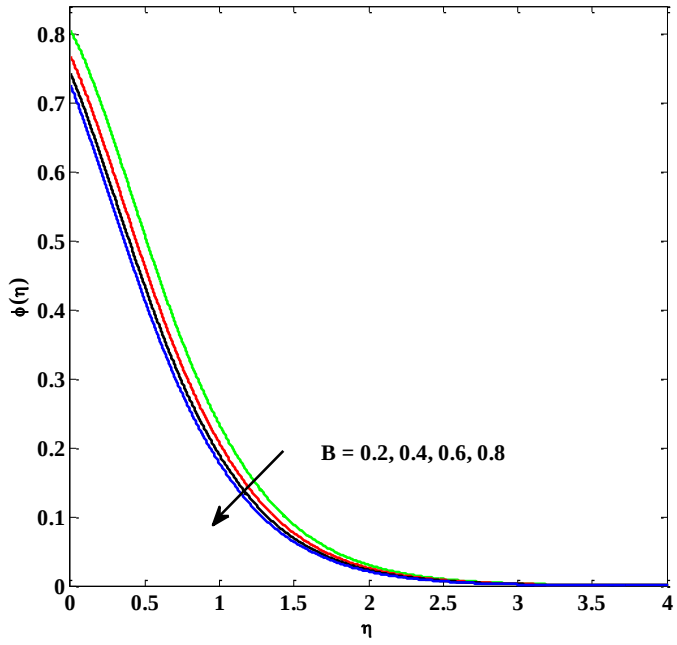

Fig. 24. $\varphi(\eta)$ for picked values of B

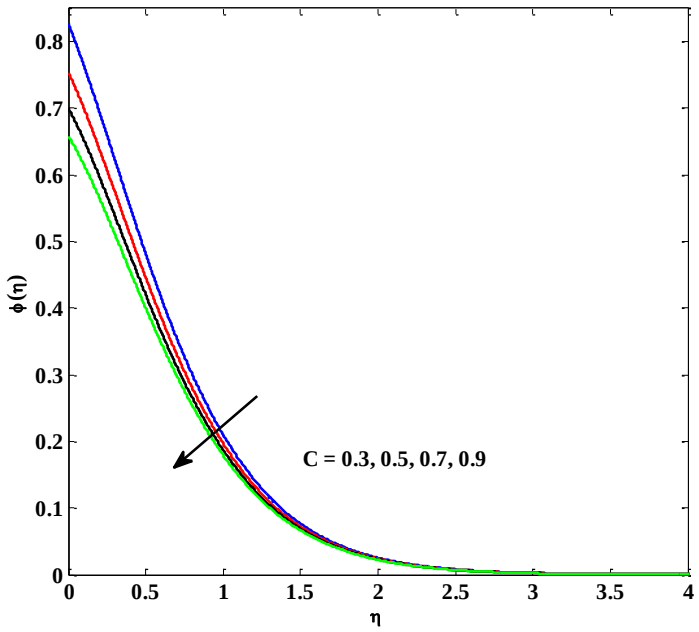

Fig. 25. $\varphi(\eta)$ for picked values of C

FINAL REMARKS:

A numerical study of Williamson nanofluid with the effect of aligned MHD passing through a stretched surface and porous medium is performed in addition to the effects of heat radiation and slips. By Kellor-Box method the influence of several flow parameter on three fluid flow profiles is represented through graphically and the major findings are as follows:

International Journal of Engineering Research & Technology (IJERT)
ISSN: 2278-0181
Vol. 12 Issue 10, October-2023

- The velocity profile decreases and the temperature, concentration profiles are increased with increase in inclined angle γ.
- Both the fluid temperature and concentration decreases on increasing thermal jump parameter B and increasing in the concentration slip parameter C, the concentration profile is decreasing.
- While an increase in the value of A reduces the velocity but opposite result reflect in heat and mass transfer gradients.
- Velocity profile would make smaller while an increase in the values of M, k.
- Enhancing the values of Williamson parameter λ, a drop in velocity field is seen along with upgradation in temperature and concentration.
- The fluid temperature gradients diminish as enhanced values of Le, Pr and reverse trend in upsurge values of Nc, R.
- The fluid concentration gradient moderate as enhanced values of Sc, Nbt.

REFERENCES:

[1] Nayak, M.K.:MHD3D flowand heat transfer analysis of nanofluid by shrinking surface inspired by thermal radiation and viscous dissipation. Int. J. Mech. Sci. **124–125**, 185–193 (2017)

[2] Marzougui, S.; Bouabid, M.; Mebarek-Oudina, F.; Abu-Hamdeh, N.; Magherbi, M.; Ramesh, K.: A computational analysis of heat transport irreversibility phenomenon in a magnetized porous channel. Int. J. Numer. Methods Heat Fluid Flow **31**(7), 2197–2222 (2021). https://doi.org/10.1108/HFF-07-2020-0418

[3] Metri, P.G.; Metri, P.G.; Abel, S.; Silvestrov, S.: Heat transfer in MHD mixed convection viscoelastic fluid flow over a stretching sheet embedded in a porous medium with viscous dissipation and non-uniform heat source/sink. Procedia Eng. **157**, 309–316 (2016)

[4] Akbar, N.; Beg, O.A.; Khan, Z.H.: Magneto-nanofluid flow with heat transfer past a stretching surface for the new heat flux model using numerical approach. Int. J. Numer.Methods Heat Fluid Flow **27**(6), 1215–1230 (2017). https://doi.org/10.1108/HFF-03-2016-0125

[5] Rashidi, M.M.; Rostami, B.; Freidoonimehr, N.; Abbasbandy, S.:Free convective heat and mass transfer for MHD fluid flow over a permeable vertical stretching sheet in the presence of the radiation and buoyancy effects. Ain Shams Eng. J. **5**, 901–912 (2014)

[6] Rashidi, M.M.; Erfani, E.: Analytical method for solving steady MHD convective and slip flow due to a rotating disk with viscous dissipation and Ohmic heating. Eng. Comput. **29**, 562–579 (2012)

[7] Khedr, M.E.M.; Chamkha, A.J.; Bayomi, M.: MHD flow of a micropolar fluid past a stretched permeable surface with heat generation or absorption. Nonlinear Anal. Model. Control **14**, 27–40(2009)

[8] Fang, T.; Zhang, J.: Closed-form exact solutions of MHD viscous flow over a shrinking sheet. Commun. Nonlinear Sci. Numer Simul. **14**, 2853–2857 (2009)

[9] Magyari, E.; Chamkha, A.J.: Exact analytical results for the thermosolutal MHD Marangoni boundary layers. Int. J. Therm. Sci. **47**, 848–857 (2008)

[10] Ishak, A.; Nazar, R.; Pop, I.: MHD boundary-layer flow due to a moving extensible surface. J. Eng. Math. **62**, 23–33 (2008)

[11] Yasin, M.H.M.; Ishak,A.; Pop, I.:MHDheat andmass transfer flow over a permeable stretching/shrinking sheet with radiation effect. J. Magn. Magn. Mater. **407**, 235–240 (2016). https://doi.org/10. 1016/j.jmmm.2016.01.087

[12] Falodun, B.O.;Omowaye,A.J.: Double-diffusiveMHDconvective flow of heat and mass transfer over a stretching sheet embedded in a thermally-stratified porous medium.World J. Eng. **16**(6), 712–724 (2019). https://doi.org/10.1108/WJE-09-2018-0306

[13] Madhusudan, S.; Sampad Kumar, P.; Swain, K.; Ibrahim, S.M.: Analysis of variable magnetic field on chemically dissipative MHD boundary layer flow of Casson fluid over a nonlinearly stretching sheet with slip conditions. Int. J. Ambient Energy (2020). https://

[14] doi.org/10.1080/01430750.2020.1831601

[15] Choi, S. U. S.: Enhancing thermal conductivity of fluids with nanoparticles. In: Proceedings of the ASME International Mechanical Engineering Congress and Exposition, San Francisco, CA, USA, pp. 99–105 (1995)

[16] Eastman, J.A.; Choi, S.U.S.; Li, S.; Yu, W.; Thompson, L.J.: nomalously increased effective thermal conductivities of ethylene glycol-based nanofluids containing copper nanoparticles. Appl. Phys. Lett. **78**(6), 718–720 (2001)

[17] Kuznetsov, A.V.; Nield, D.A.: Natural convective boundary-layer flow of a nanofluid past a vertical plate. Int. J. Therm. Sci. **49**, 243–247 (2010)

[18] Anwar, M.I.; Khan, I.; Hussanan, A.; Salleh, M.Z.; Sharidan, S.:Stagnation-point flow of a nanofluid over a nonlinear stretching sheet. World Appl. Sci. J. **23**, 998 (2013)

[19] Azimi, M.; Riazi, R.: Heat transfer of GO-water nanofluid flow between two parallel disks. Propuls. Power Res. **4**, 23–50 (2015)

[20] Bhargava, R.; Goyal, M.; Pratibha: An efficient hybrid approach for simulating MHD nanofluid flow over a permeable stretching sheet. Springer Proc. Math. Stat. **143**, 701–714 (2015)

[21] Raza, J.; Mebarek-Oudina, F.; Mahanthesh, B.: Magnetohydrodynamic flow of nano Williamson fluid generated by stretching plate with multiple slips. Multidiscip. Model. Mater. Struct. **15**(5), 871–894 (2019). https://doi.org/10.1108/MMMS-11-2018-0183

[22] Khan, U.; Zaib, A.; Mebarek-Oudina, F.: Mixed convective magneto flow of SiO2-MoS2/C2H6O2 hybrid nanoliquids through a vertical stretching/shrinking wedge: Stability analysis.Arab. J. Sci. Eng. **45**(11), 9061–9073 (2020). https://doi.org/10.1007/s13369-

[23] 020-04680-7

[24] Chamkka, A.J.; Aly, A.M.; Al-Mudhaf, H.: Laminar MHD mixed convection flow of a nanofluid along a stretching permeable surface in the presence of heat generation or absorption effects. Int. J. Microscale Nanoscale Therm. Fluid Transp. Phenom. **2**, 51–70 (2011)

[25] Turkyilmazoglu, M.: Exact analytical solutions for heat and mass transfer of MHD slip flowin nanofluids. Chem. Eng. Sci. **84**, 182–187 (2012)

[26] Wubshet, I.; Shankar, B.:MHD boundary layer flow and heat transfer of a nanofluid past a permeable stretching sheet with velocity, thermal and solutal slip boundary conditions. Comput. Fluids **75**, 1–10 (2013)

[27] Nagendra, N.; Amanulla, C.H.; Sudhakar Reddy, M.; Ramachandra, P.V.: Hydromagnetic flow of heat and mass transfer in a nano Williamson fluid past a vertical plate with thermal and momentum slip effects: numerical study. Nonlinear Eng. **8**, 127–144 (2019)

[28] Garoosi, F.; Jahanshaloo, L.; Rashidi, M.M.; Badakhsh, A.; Ali M.E.: Numerical simulation of natural convection of the nanofluid in heat exchangers using a Buongiorno model. Appl. Math. Comput. **254**, 183–203 (2015)

[29] Konda, J.R.; Madhusudhana Reddy, N.P.; Konijeti, R.; Dasore, A.: Effect of non-uniform heat source/sink on MHD boundary layer flow and melting heat transfer of Williamson nanofluid in porous medium. Multidiscip. Model. Mater. Struct. **15**, 452–472 (2019).

[30] https://doi.org/10.1108/MMMS-01-2018-0011

[31] Yahaya, S.D.; Zainal, A.A.; Zuhaila, I.; Faisal, S.: Hydromagnetic slip flow of nanofluid with thermal stratification and convective heating. Aust. J. Mech. Eng. **18**(2), 147–155 (2020). https://doi. org/10.1080/14484846.2018.1432330

[32] Acharya, N.; Das, K.; Kundu, P.K.: Influence of multiple slip and chemical reaction on radiative MHD Williamson nanofluid flow in porous medium: a computational framework. Multidiscip. Model. Mater. Struct. **15**(3), 630–658 (2019). https://doi.org/10. 1108/MMMS-08-2018-0152

[33] Arabian Journal for Science and Engineering

[34] Mishra, S.R.; Mathur, P.: Williamson nanofluid flow through porous medium in the presence of melting heat transfer boundary condition: semi-analytical approach. Multidiscip. Model. Mater. Struct. **17**(1), 19–33 (2021). https://doi.org/10.1108/MMMS-12- 2019-0225

[35] Asogwa, K.; Mebarek-Oudina, F.; Animasaun, I.: Comparative investigation of water-based Al2O3 nanoparticles through water based CuO nanoparticles over an exponentially accelerated radiative riga plate surface via heat transport. Arab. J. Sci. Eng. (2021).

[36] https://doi.org/10.1007/s13369-021-06355-3

[37] Warke, A.S.; Ramesh, K.; Mebarek-Oudina, F.; Abidi, A.: Numerical investigation of nonlinear radiation with magnetomicropolar stagnation point flow past a heated stretching sheet. J. Therm.Anal. Calorim. (2021). https://doi.org/10.1007/s10973-021-10976-z

[38] Mahanthesh, B.; Gireesha, B.J.; Animasaun, I.L.: Exploration of non-linear thermal radiation and suspended nanoparticles effects on mixed convection boundary layer flow of nanoliquids on a melting vertical surface. J. Nanofluids **7**(5), 833–843 (2018)

[39] Mabood, F.; Ibrahim, S.M.; Lorenzini, G.; Lorenzini, E.: Radiation effects on Williamson nanofluid flow over a heated surface with magnetohydrodynamics. Int. J. Heat Technol. **35**(1), 196–204 (2017)

[40] Bhatti, M.M.; Rashidi, M.M.: Effects of thermo-diffusion and thermal radiation on Williamson nanofluid over a porous shrinking/stretching sheet. J. Mol. Liq. **221**, 567–573 (2016)

[41] Krishnamurthy, M.R.; Gireesha, B.J.; Prasannakumara, B.C.; Gorla, R.S.R.: Thermal radiation and chemical reaction effects on boundary layer slip flow and melting heat transfer of nanofluid induced by a nonlinear stretching sheet. Nonlinear Eng. **5**(3), 147–159 (2016)

[42] Pal, D.; Roy, N.; Vajravelu, K.: Thermophoresis and Brownian motion effects on magneto-convective heat transfer of viscoelastic nanofluid over a stretching sheet with nonlinear thermal radiation. Int. J. Ambient Energy (2019). https://doi.org/10.1080/01430750.

[43] 2019.1636864

[44] Ghadikolaei, S.S.; Hosseinzadeh, K.; Ganji, D.D.: Investigation on Magneto Eyring-Powell nanofluid flow over inclined stretching cylinder with non-linear thermal radiation and Joule heating effect. World J. Eng. **16**(1), 51–63 (2019). https://doi.org/10.1108/WJE- 06-2018-0204

[45] Almakki,M.; Mondal, H.; Sibanda, P.: Entropy generation in magneto nanofluid flow with Joule heating and thermal radiation. World J. Eng. **17**(1), 1–11 (2020). https://doi.org/10.1108/WJE-06-2019-0166

[46] Gao, T.; Li, C.; Yang, M.; Zhang, Y.; Jia, D.; Ding, W.; Debnath S.; Yu, T.; Said, Z.; Wang, J.: Mechanics analysis and predictive force models for the single-diamond grain grinding of carbon fiber reinforced polymers using CNT nano-lubricant. J. Mater. Process. Technol. **290**, 116976 (2021). https://doi.org/10.1016/j.jmatprotec. 2020.116976

[47] Pushpa,B.V.; Sankar, M.;Mebarek-Oudina, F.: Buoyant convective flow and heat dissipation of Cu–H2O nanoliquids in an annulus through a thin baffle. J. Nanofluids **10**(2), 292–304 (2021). https://doi.org/10.1166/jon.2021.1782

[48] Wang, X.; Li, C.; Zhang, Y.; Said, Z.; Debnath, S.; Sharma, S.; Yang, M.; Gao, T.: Influence of texture shape and arrangement on nanofluid minimum quantity lubrication turning. Int. J. Adv. Manuf. Technol. **119**, 631–646 (2022). https://doi.org/10.1007/s00170-021-08235-4

International Journal of Engineering Research & Technology (IJERT)
ISSN: 2278-0181
Vol. 12 Issue 10, October-2023

[49] Dadheech, P.K.; Agrawal, P.; Mebarek-Oudina, F.; Abu-Hamdeh, N.; Sharma, A.: Comparative heat transfer analysis of MoS2/C2H6O2 and MoS2–SiO2/C2H6O2 nanofluids with natural convection and inclined magnetic field. J.Nanofluids **9**(3), 161–167 (2020). https://doi.org/10.1166/jon.2020.1741

[50] Chabani, I.; Mebarek-Oudina, F.; Ismail, A. I.: MHD flow of a hybrid nano-fluid in a triangular enclosure with zigzags and an elliptic obstacle. Micromachines **13**(2), 224 (2022). https://doi.org/ 10.3390/mi13020224

[51] Djebali, R.; Mebarek-Oudina, F.; Choudhari, R.: Similarity solution analysis of dynamic and thermal boundary layers: further formulation along a vertical flat plate. Phys. Scr. **96**(8), 085206 (2021). https://doi.org/10.1088/1402-4896/abfe31

[52] Marzougui, S.; Mebarek-Oudina, F.; Mchirgui, A.; Magherbi, M.: Entropy generation and heat transport of Cu-water nanoliquid in porous lid-driven cavity through magnetic field. Int. J. Numer. Methods Heat Fluid Flow (2021). https://doi.org/10.1108/HFF-04-2021-0288

[53] Hayat, T.;Abbas, Z.; Javed, T.: Mixed convection flowof amicropolar fluid over a non-linearly stretching sheet. Phys. Lett. A **372**(5), 637–647 (2008)

[54] KhoYap, B.; Abid, H.; Muhammad Khairul, A.M.; Mohd Zuki, S.:Heat and mass transfer analysis on flow of Williamson nanofluid with thermal and velocity slips: Buongiorno model. Propuls. Power Res. **8**(3), 243–252 (2019)

